Supplementary Information (SI) for ChemComm.

Supporting Information

# Terminal-selective Healing of Perovskite Crystals for Air-Fabricated High-performance Flexible Perovskite Solar Cells

Shendong Xu,[a] Yuli Tao,[b] Ke Yang,*[a] Yongtao Li,*[c] Haiying Zheng,[d] Guozhen Liu*[e] and Xu Pan*[b]

[a]School of Carbon Neutrality Science and Engineering, Anhui University of Science and Technology, Hefei 231131, P. R. China. E-mail: 2023183@aust.edu.cn (K. Yang)

[b]Key Laboratory of Photovoltaic and Energy Conservation Materials, Institute of Solid State Physics, Hefei Institutes of Physical Science, Chinese Academy of Sciences, Hefei 230031, P. R. China. E-mail: xpan@rntek.cas.cn (X. Pan)

[c]School of Materials Science and Engineering, Anhui University of Technology, Maanshan 243002, P. R. China. E-mail: liyongtao@ahut.edu.cn (Y. Li)

[d]School of Materials Science and Engineering, Dalian Jiaotong University, Dalian 116028, P. R. China

[e]State Key Laboratory of Fine Chemicals, School of Chemistry, Dalian University of Technology, Dalian 116024, P. R. China. E-mail: gzliu@dlut.edu.cn (G. Liu)

# Experimental section

## Materials

**Basic materials**: Methylammonium iodide (MAI), formamidinium iodide (FAI, 99.9%), methylammonium bromine (MABr), methylamine Chloride (MACl) and lead(II) iodide ($PbI_2$, 99.999%), lead (II) bromide ($PbBr_2$, >98%) and cesium iodide (CsI, >99%) both purchased from Advanced Election Technology Co. Spiro-MeOTAD (99.86%) was purchased from Xi'an Polymer Light Technology manufacturers. The $SnO_2$ colloid precursor (tin (IV) oxide, 15% in $H_2O$ colloidal dispersion) was obtained from Alfa Aesar. DMSO (dimethylsulfoxide 99.50%), DMF (N,N-dimethylformamide 99.99%), chlorobenzene and isopropanol (IPA) from Sinopharm and Sigma Aldrich.

**Special materials**: The hexadecyltrimethylammonium hexafluorophosphate ($HTAPF_6$) and hexadecyltrimethylammonium tetrafluoroborate ($HTABF_4$) were purchased from aladdin.

**Electrode materials**: ITO-PEN also purchased from Advanced Election Technology Co. Au (99.99%) was purchased from ZhongNuo Advanced Material Technology or any other company as long as the purity is above 4 nines (99.99%).

All the commercial materials were used as received without further purification.

## Flexible Perovskite Solar Cells (f-PSCs) Structure

Device structure is PEN-ITO/$SnO_2$/perovskite/ spiro-MeOTAD/Au.

## Preparation of Perovskite Precursor Solution

The perovskite precursor solutions (The concentration of lead ions is 1.6 M) of $(FAPbI_3)_{0.925}(MAPbBr_3)_{0.05}(CsPbI_3)_{0.025}$ was fabricated by dissolving the corresponding amount of $PbI_2$, PbBr, FAI, CsI, MAI, MABr, MACI powders in anhydrous N,N-dimethylformamide (DMF) and dimethyl sulfoxide (DMSO) mixed solvent (DMF:DMSO = 4:1) with stirring at 25 °C for 60 min. (The following text is referred to as the perovskite precursor)

## Single-junction Flexible Perovskite Solar Cells (PSCs) Fabrication

### Flexible substrate slicing and cleaning

Firstly, the etched PEN-ITO (The PEN-ITO film was cut into uniform pieces of 1.5 cm × 2 cm) was cleaned by using the detergent for 15 min, ultrapure water for 20 min, and ethanol for 20 min, sequentially.

### Preparation of the electronic transport layer

And then, the PEN-ITO was treated through an ultraviolet ozone (UVO) for 30 min. The $SnO_2$ films were prepared by spin-coating the above $SnO_2$ colloidal solution (100 μL) on the etched ITO substrates at 4000 rpm for 50 s and then the $SnO_2$ films was annealed at 100 ℃ for 60 min. Afterwards, all the $SnO_2$ films were exposed to UVO for 30 min.

### Preparation of the photoactive layer

The perovskite layers were coated by spin coating 1.6M perovskite precursor solutions in dry air(humidity was kept at about 5% RH) flowing glovebox.

Chlorobenzene (100 μL) was dropwise added on the substrate during the spin-coating step 15s before the end of the total procedures. The substrate was sintered at 150 °C for 15 min on a hotplate.

### Preparation of the pre-sewing layer

After cooling to room temperature, $HTAPF_6$ or $HTABF_4$ solutions with different concentrations were respectively spin-coated on the perovskite layer with 3000 r.p.m. for 20 s and heated at 100 °C for 5~10 min.

### Preparation of the hole transport layer

Subsequently, the hole-transporting material (HTM) solution was deposited on the perovskite layer by spin coating which was comprised of spiro-OMeTAD (80 mg), 4-tert-butylpyridine, cobalt(III) salt and lithium bis-(trifluoromethanesulfonyl)imide and in chlorobenzene solvent.

### Preparation of the metal electrode layer

Finally, the films were dried under vacuum before completing the device fabrication process by thermal evaporating 80 nm of Au on top of the HTM layer.

## Flexible Perovskite Solar Cells (F-PSCs) Module Fabrication

Compared with the single-junction F-PSCs fabrication, the fabrication of each functional layer remains unchanged except for the amount of solution. For the 4 $cm^2$ and 10 $cm^2$ micro modules, the size of the PEN-ITO substrate used is both 4.5×4.5 $cm^2$. The difference lies in the number of sub-cells, which are 4 and 6 respectively. The precise effective area is controlled by the mask.

For the 4.5 × 4.5 $cm^2$ module, 800 μl perovskite solution was used. Laser-patterning lines (P1, P2, and P3) were accomplished by the 355 nm laser beam with a power of 5 W, a current of 1A, a scribing speed of 550 mm $s^{-1}$, and a pulse width of 20 μs. The line widths of P1, P2, and P3 are about 70, 100, and 100 μm, respectively. The line spacing between P1 and P2, and P2 and P3 is about 100 μm.

## DFT calculations

**Adsorption energy**: The adsorption energy ($E_{ads}$) of the complex formed between molecules A and B was calculated using the following equation: $E_{ads} = E_{complex} - (E_A - E_B)$, where $E_{complex}$ is the total energy of molecular complexes A and B. $E_A$ and $E_B$ are the total energies of the isolated molecules A and B, respectively. The whole calculation is based on the VASP platform, and its specific parameters and boundary conditions are set according to the previously reported articles.[1-3]

**Electrostatic potential**: The electrostatic potential (ESP) of hexadecyltrimethylammonium hexafluorophosphate ($HTAPF_6$) and hexadecyltrimethylammonium tetrafluoroborate ($HTABF_4$) were calculated by Gaussian 16 package.[1]

## Characterization

**Photovoltaic performance**: PCEs and *J-V* curves were obtained via using a solar simulator (Newport, Oriel Class A, 91195A) and a source meter (Keithley 2420).

IPCE with a wavelength range from 300 to 900 nm were tested with dual Xenon/quartz halogen light source (PV Measurements, Inc.), and measured in DC mode with no bias light used. The solar simulator with 100 mW/cm$^2$ illumination AM 1.5G was calibrated via a Si-reference cell which was certified by NREL. Via masking a black mask, the devices retained an active area of 0.09 cm$^2$.

All the tests of the micro-modules were conducted using masks to control the actual effective working area of the solar cells. In the device with an area of 0.09 cm$^2$, the effective area is controlled by adjusting the area of the evaporation electrode.

**Morphological observation**: SEM images were performed on a field-emission scanning electron microscope (Gemini SEM 500, Zeiss, Germany) with high-resolution.

**Absorption spectrum**: The Ultraviolet–visible absorption spectra were obtained from ultraviolet-vis (UV-vis) spectrophotometer(U-3900H, HITACHI, Japan).

**Carrier dynamics**: Steady-state PL spectra were obtained from a spectrofluorometer (photon technology international). The exciting wavelength was 475 nm and excited by a standard 450 W xenon CW lamp and analyzed by the software Fluorescence. The time-resolved PL experiments were performed with the same Fluorescence Lifetime Spectrofluorometer using a pulsed source at 450 nm (the illumination source is a pulsed nitrogen dye laser) and the signal was recorded at 770 nm by the Time Correlated Single Photon Counting (TCSPC) technique.

**Photoelectron Spectroscopy**: X-ray photoelectron spectra (XPS) and Ultraviolet photoelectron spectra (UPS) measurements were collected with Thermo ESCALAB

250Xi system. X-ray diffraction (XRD) patterns with 2θ range from 5° to 50° were carried out on a Rigaku smartlab 9KW with Cu Kα radiation. Depth-dependent grazing incident X-ray diffraction (GIXRD) patterns with Inclination angles (Ψ) range from 0° to 30° (step 5° ) were carried out on a Small Angle X-ray scatterer (SAXSpoint2.0). Contact angles were conducted on an OCA15EC contact angle measuring instrument (Dataphysics, Germany) with a drop of ultrapure water.

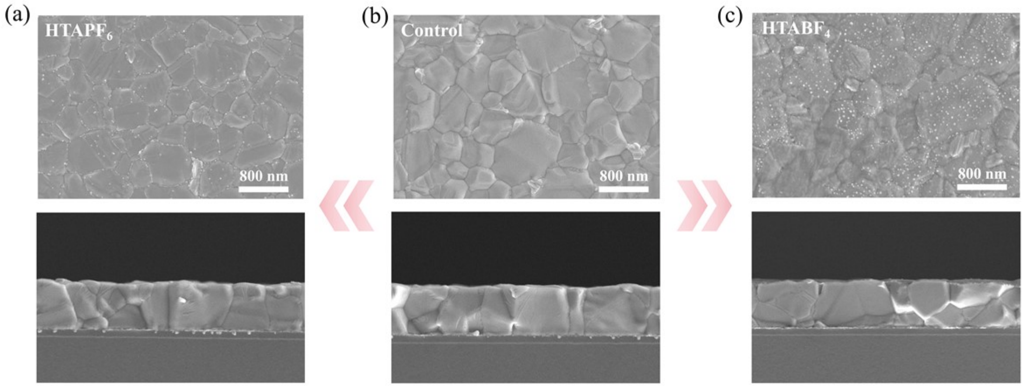

**Fig. S1** Top-view and cross-sectional SEM images of (a) $HTAPF_6$-treated, (b) control and (c) $HTABF_4$-treated perovskite films.

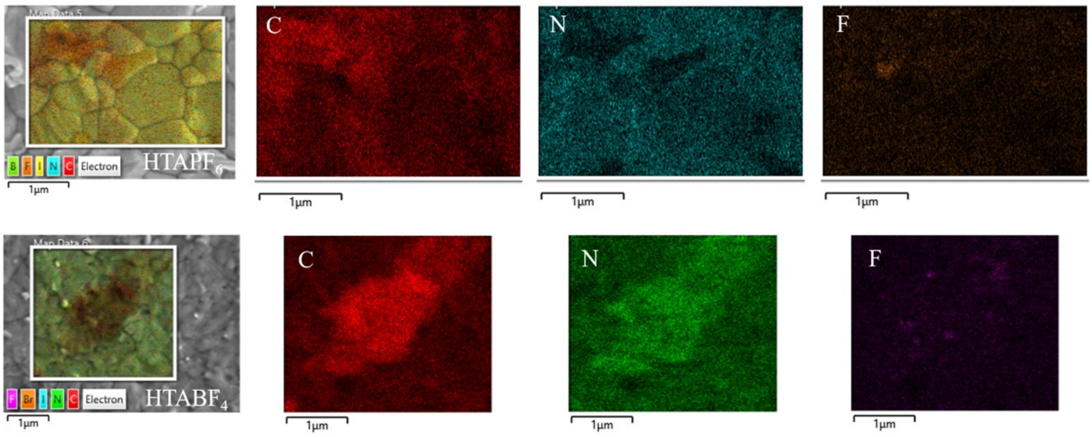

**Fig. S2** EDS images of $HTAPF_6$-treated and $HTABF_4$-treated perovskite films.

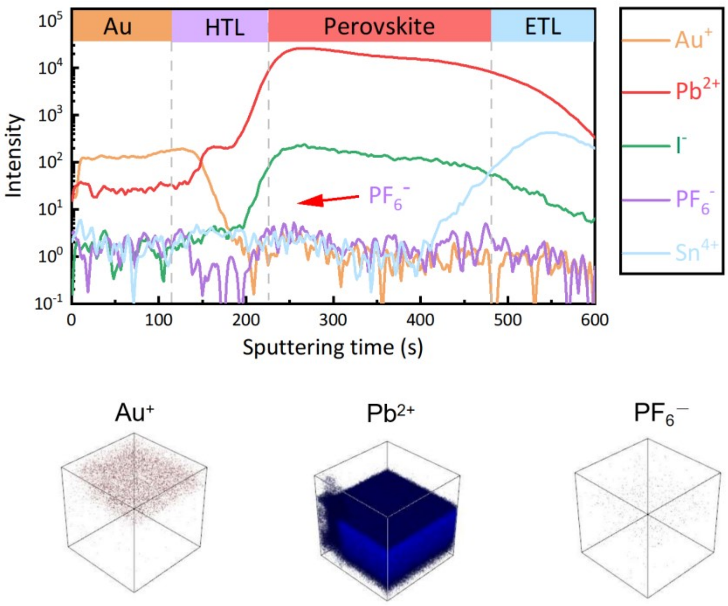

**Fig. S3** Tof-sims for 3D renders of $HTAPF_6$-treated perovskite films.

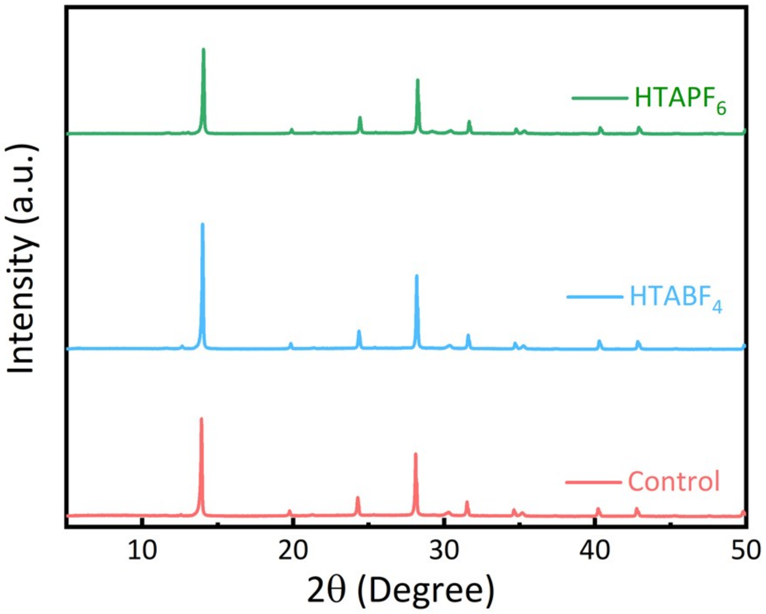

**Fig. S4** XRD patterns for control and $HTAPF_6$/$HTABF_4$-treated perovskite films.

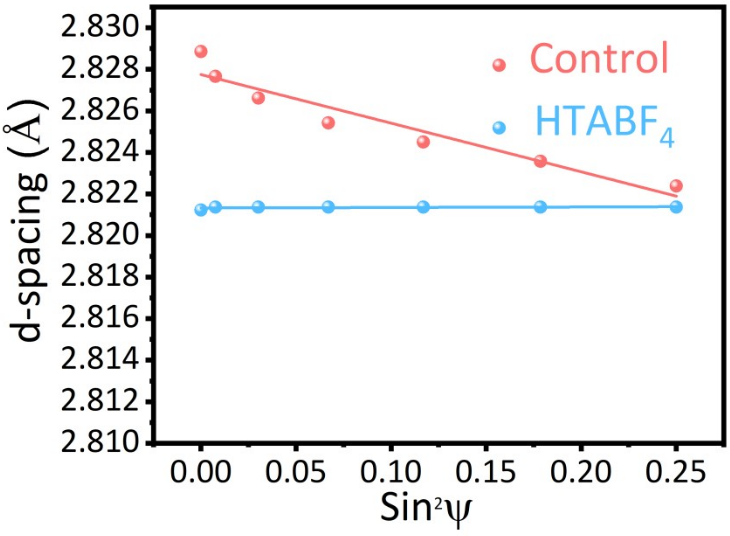

**Fig. S5** 2θ-sin$^2$(Ψ) curve of control and HTABF$_4$-treated perovskite films obtained from GIXRD.

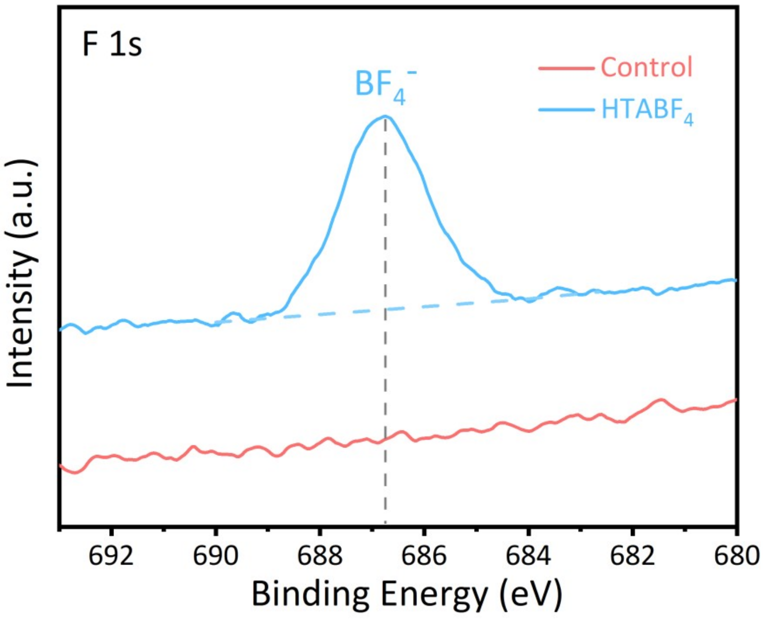

**Fig. S6** XPS characterization of F element of the control and HTABF$_4$-treated films.

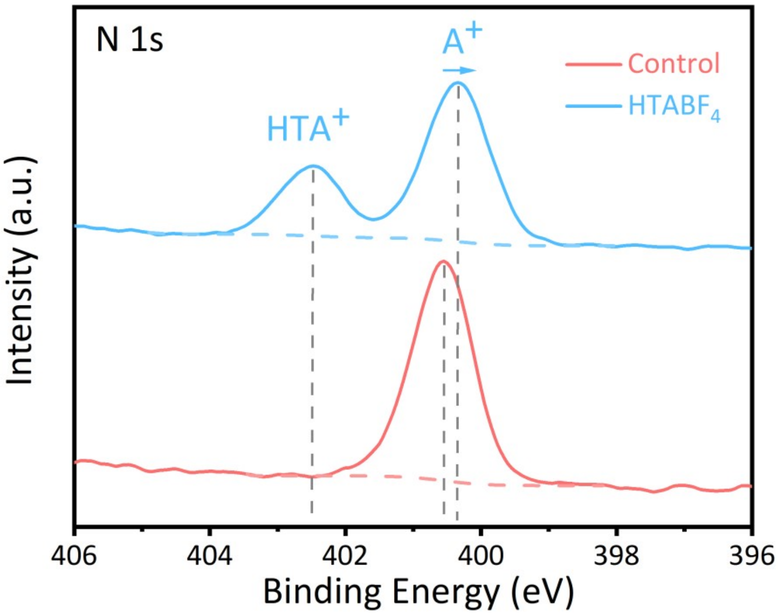

**Fig. S7** XPS characterization of N element of the control and HTABF$_4$-treated films.

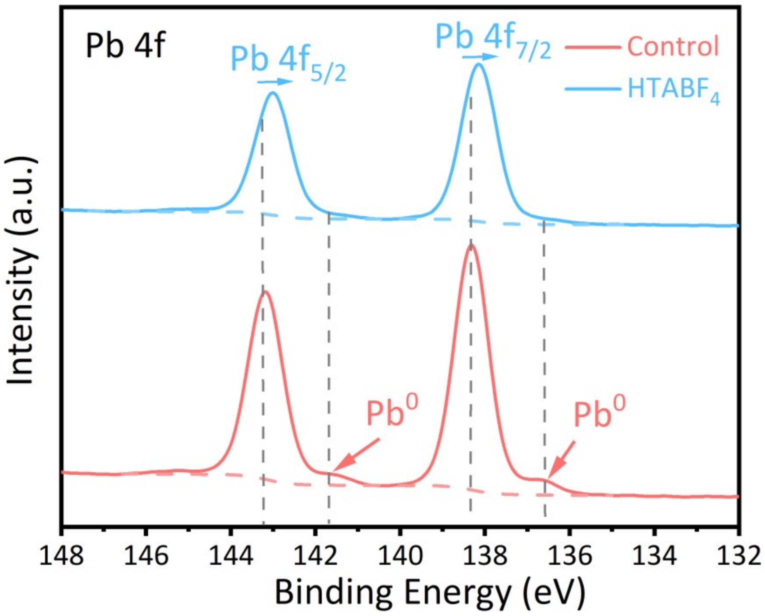

**Fig. S8** XPS characterization of Pb element of the control and HTABF$_4$-treated films.

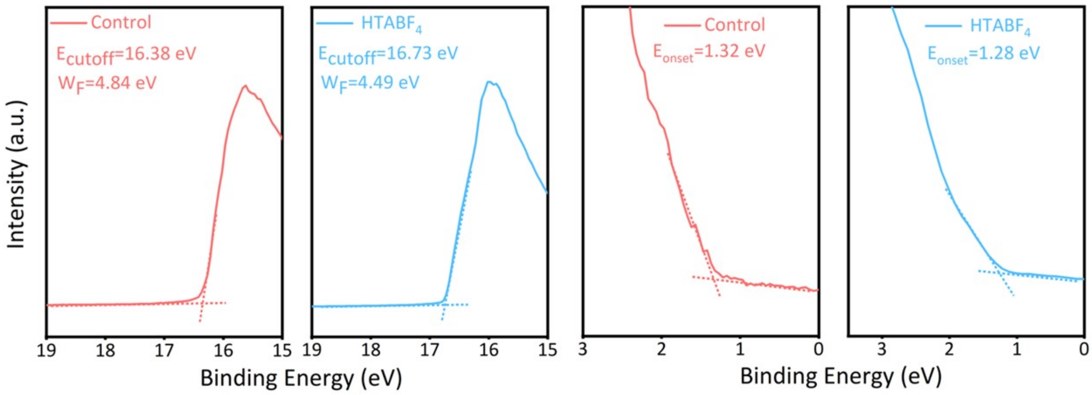

**Fig. S9** UPS spectra of control and HTABF$_4$-treated perovskite films.

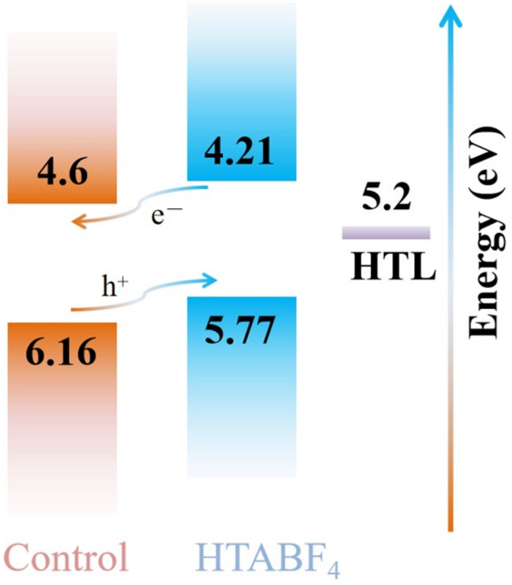

**Fig. S10** Schematic diagram of the energy level in control and HTABF$_4$-treated perovskite films.

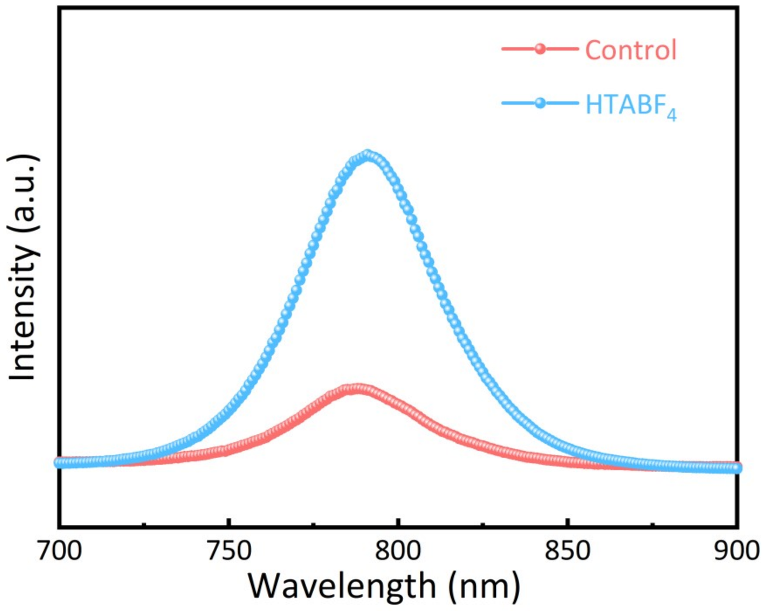

**Fig. S11** Steady-state PL spectra for control and HTABF$_4$-treated perovskite films.

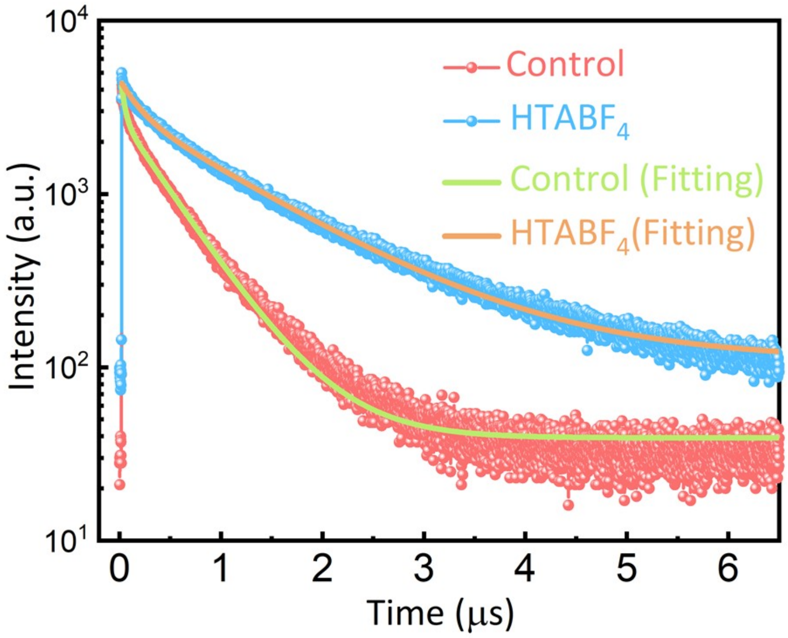

**Fig. S12** Time-resolved PL spectra for control and HTABF$_4$-treated perovskite films.

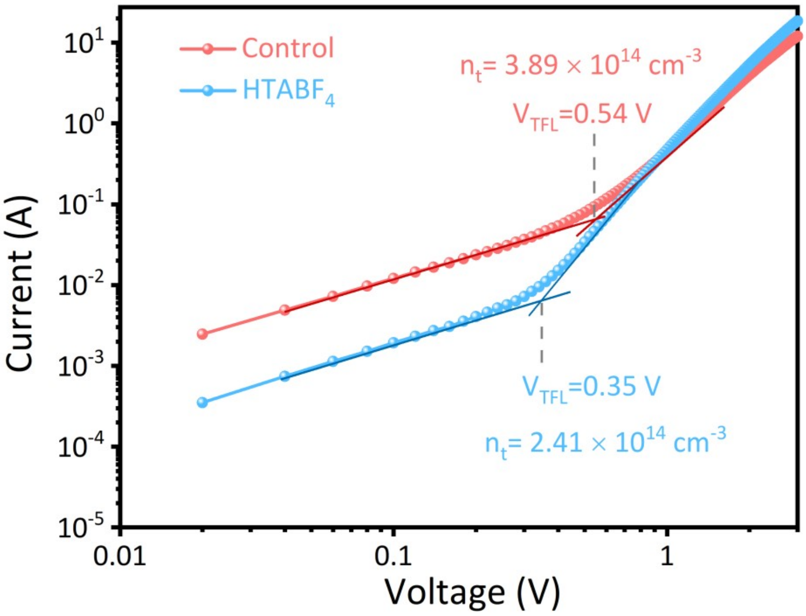

**Fig. S13** Space charge limited current (SCLC) curves of control device and HTABF$_4$-treated device.

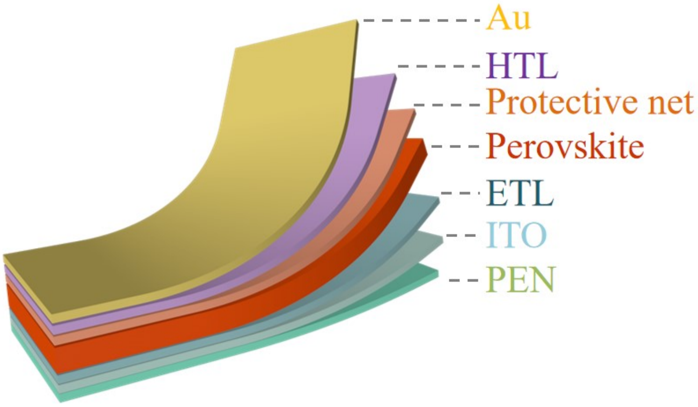

**Fig. S14** Schematic diagram of flexible perovskite solar cells.

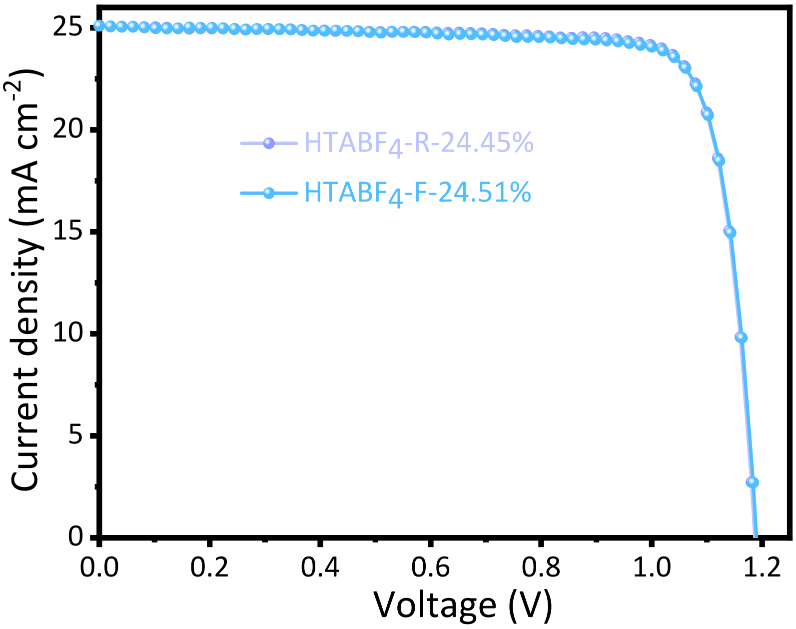

**Fig. S15** *J-V* curves with reverse and forward scans of champion devices with HTABF$_4$-treated.

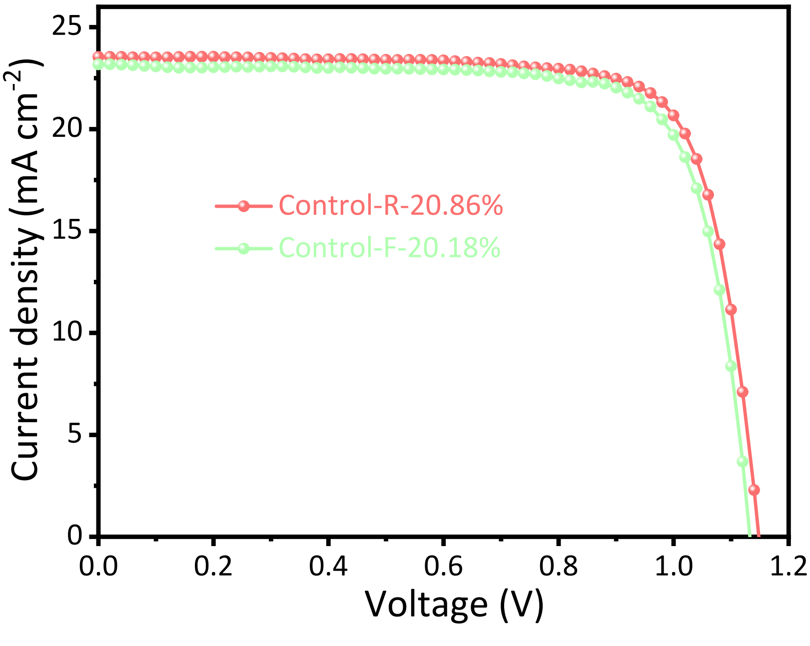

**Fig. S16** *J-V* curves with reverse and forward scans of control device.

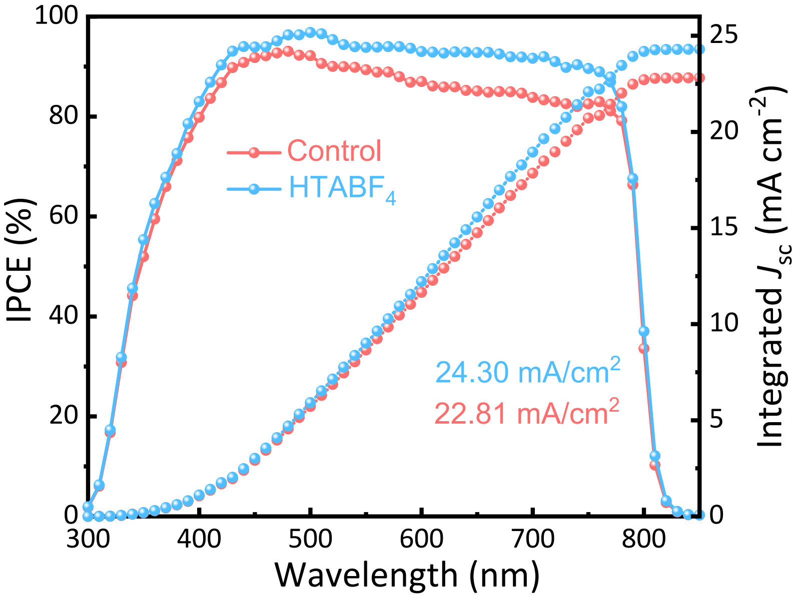

**Fig. S17** IPCE spectra of the champion devices without and with HTABF$_4$-treated.

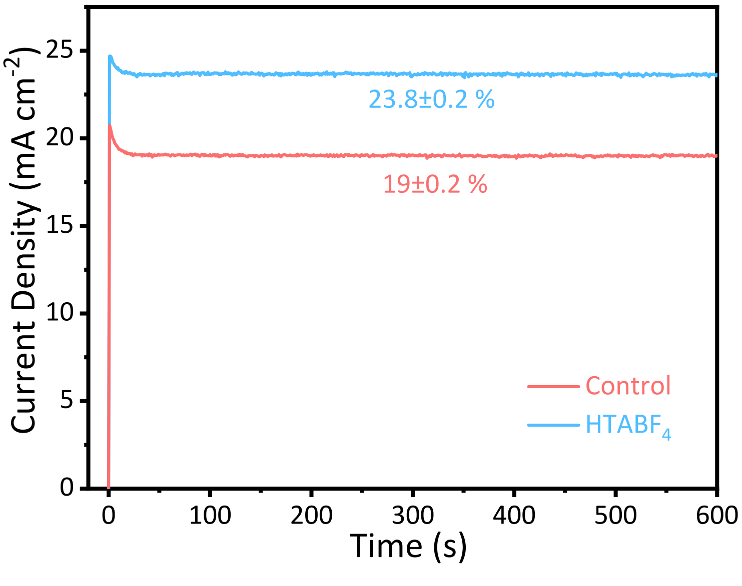

**Fig. S18** Steady-state output during measurements of the PCE for the PSCs.

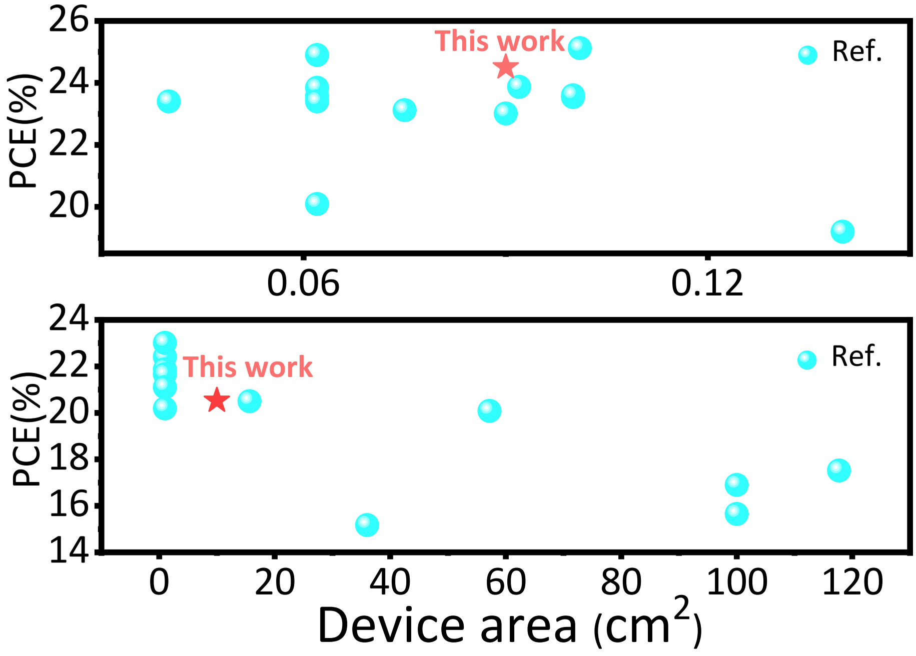

**Fig. S19** Statistical diagram of the device areas (0 to 120 cm$^2$) and PCE values obtained from the recently reported high-performance flexible perovskite solar cells.

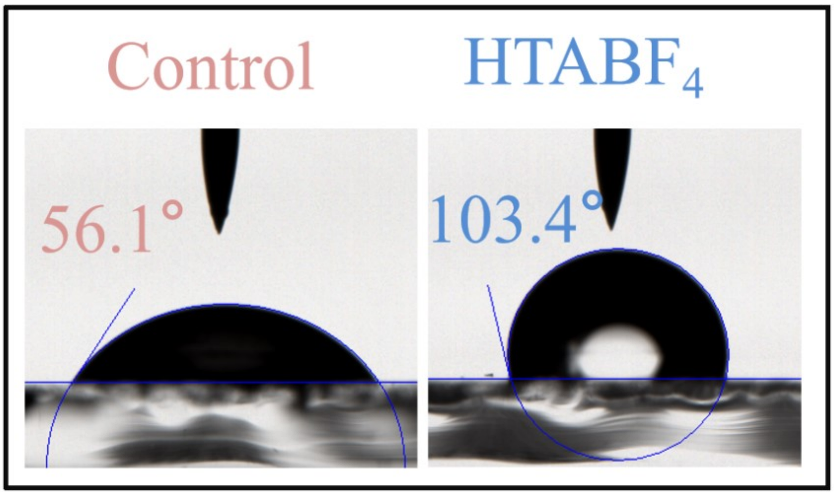

**Fig. S20** Contact angle measurement for control and HTABF$_4$-treated perovskite films.

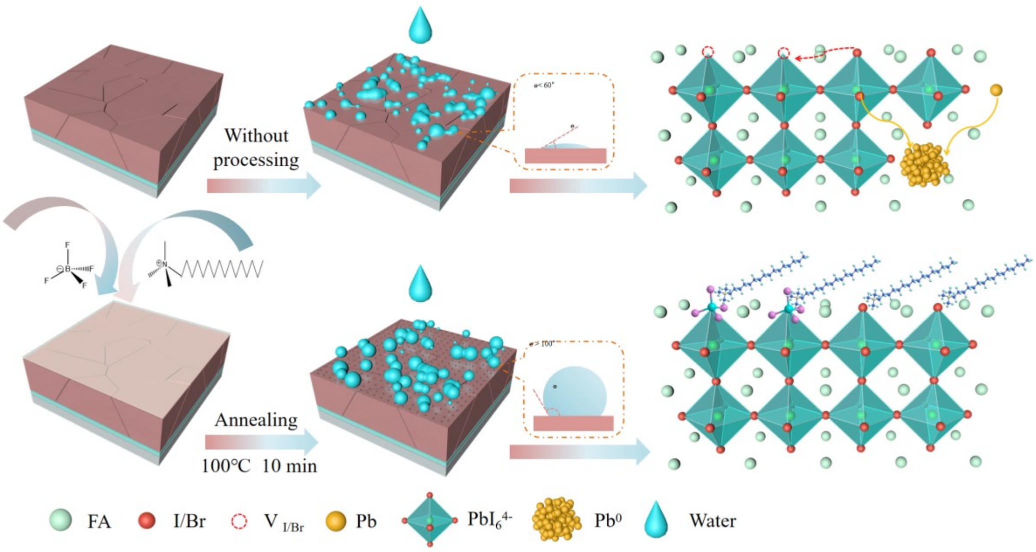

**Fig. S21** Schematic diagram of the surface hydrophobic mechanism of perovskite films.

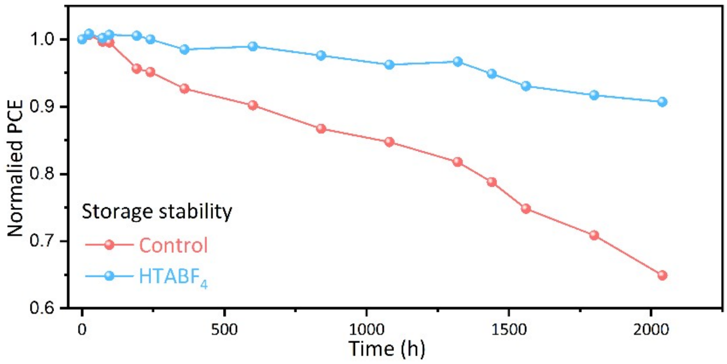

**Fig. S22** Environmental stability of unencapsulated F-PSCs with HTABF4-treated (50% relative humidity at room temperature).

**Table** S1.

Fitted results of TRPL curves in Figure 4b using a double exponential decay equation of $I(t) = I_0 + A_1\exp(-t/\tau_1) + A_2\exp(-t/\tau_2)$, where $\tau_1$ and $\tau_2$ represent fast and slow decay time constants, respectively, to quantify the carrier lifetime decay. The average time constant ($\tau_{\mathrm{ave}}$) is calculated using relation $\tau\mathrm{ave} = (A_1\tau_1^2+A_2\tau_2^2)/(A_1\tau_1+A_2\tau_2)$.

| Devices | $A_1$ | $\tau_1$ [ns] | $A_2$ | $\tau_2$ [ns] | $\tau_{ave}$ [ns] |
|---|---|---|---|---|---|
| **Control** | 2635.01 | 39.08 | 2760.73 | 495.86 | **463.96** |
| **HTABF$_4$** | 1533.73 | 182.30 | 2945.96 | 1200.97 | **1126.36** |

**Table** S2.

Photovoltaic parameters of the control and HTABF$_4$-treated devices in RS under simulated AM 1.5G one sun illumination of 100 mW/cm$^2$.

| Devices | $J_{\mathrm{sc}}$ (mA/cm$^2$) | $V_{\mathrm{oc}}$ (V) | FF (%) | PCE (%) |
|---|---|---|---|---|
| **Control** | **23.55** | **1.15** | **77.21** | **20.86** |
| **HTABF$_4$** | **25.11** | **1.185** | **82.36** | **24.51** |

**Table** S3.

Photovoltaic parameters of the HTABF$_4$-treated devices in RS and FS under simulated AM 1.5G one sun illumination of 100 mW/cm$^2$.

| Devices | $J_{\mathrm{sc}}$ (mA/cm$^2$) | $V_{\mathrm{oc}}$ (V) | FF (%) | PCE (%) |
|---|---|---|---|---|
| **HTABF$_4$-F** | **25.10** | **1.19** | **82.01** | **24.45** |
| **HTABF$_4$-R** | **25.11** | **1.185** | **82.36** | **24.51** |

**Table** S4.

Photovoltaic parameters of the control devices in RS and FS under simulated AM 1.5G one sun illumination of 100 mW/cm$^2$.

| Devices | $J_{sc}$ (mA/cm$^2$) | $V_{oc}$ (V) | FF (%) | PCE (%) |
|---|---|---|---|---|
| **Control-F** | **23.18** | **1.13** | **76.96** | **20.18** |
| **Control-R** | **23.55** | **1.15** | **77.21** | **20.86** |

**Table** S5.

Photovoltaic parameters of the HTABF$_4$-treated module (4cm$^2$) devices in RS and FS under simulated AM 1.5G one sun illumination of 100 mW/cm$^2$.

| Modules（4） | $J_{sc}$ (mA/cm$^2$) | $V_{oc}$ (V) | FF (%) | PCE (%) |
|---|---|---|---|---|
| **HTABF$_4$-F** | **6.22** | **4.58** | **79.06** | **22.43** |
| **HTABF$_4$-R** | **6.22** | **4.59** | **79.42** | **22.68** |

**Table** S6.

Photovoltaic parameters of the HTABF$_4$-treated module (10cm$^2$) devices in RS and FS under simulated AM 1.5G one sun illumination of 100 mW/cm$^2$.

| Modules（10） | $J_{sc}$ (mA/cm$^2$) | $V_{oc}$ (V) | FF (%) | PCE (%) |
|---|---|---|---|---|
| **HTABF$_4$-F** | **3.92** | **6.92** | **73.53** | **19.94** |
| **HTABF$_4$-R** | **3.93** | **6.95** | **75.23** | **20.53** |

**Table S7**. Summary of recently reported flexible perovskite solar cells.

| **Summary of Air-Processed Flexible Perovskite Solar Cells** | | | | |
|---|---|---|---|---|
| **Device structure** | **Device fabrication** | **Small-area (PCE%)** | **Large-area (PCE%)** | **Periodical information** |
| n-i-p | spin-coating | 0.092cm$^2$(23.87) | 1cm$^2$(22.41) | Advanced Materials, 2025, 37, 2418791 |
| n-i-p | spin-coating | Not specified (24.43) | 1cm$^2$(23.01) | Nature Communications, 2025, 16.1: 1771 |
| n-i-p | blade-coating | 0.1cm$^2$(23.54) | 57.2cm$^2$(20.08) | Joule, 2025, 9.5 |
| p-i-n | spin-coating | 0.14cm$^2$(19.2) | / | Chemical Engineering Journal, 2025, 164371 |
| n-i-p | blade-coating | / | 100cm$^2$(15.65) | Advanced Functional Materials, 2025, 35, 2424191 |
| n-i-p | blade-coating | 0.101cm$^2$(25.12) | 100cm$^2$(16.99) | Advanced Materials, 2025, 37, 2417779 |
| n-i-p | spin-coating | 0.075cm$^2$(23.12) | / | ACS Nano, 2025, 19, 4867-4875 |
| n-i-p | spin-coating | 0.062cm$^2$(24.9) | 15.64cm$^2$(20.5) | Advanced Materials, 2024, 36, 2403531 |
| n-i-p | blade-coating | 0.09cm$^2$(23.01) | 117.7cm$^2$(17.52) | Energy Environmental Science, 2024, 17, 7069-7080 |
| n-i-p | spin-coating | 0.04cm$^2$(23.4) | / | Nano-Micro Letter, 2024,16, 178 |
| n-i-p | spin-coating | 0.062cm$^2$(20.09) | / | Advanced Functional Materials, 2024, 34, 2406354 |
| n-i-p | spin-coating | 0.062cm$^2$(23.57) | 1.004cm$^2$(21.87) | ACS Energy Letter, 2023, 8, 3750-3759 |
| n-i-p | spin-coating | 0.062cm$^2$(23.84) | 1.004cm$^2$(21.66) | Advanced Materials, 2023, 35, 2300513 |
| n-i-p | spin-coating | 0.062cm$^2$(23.4) | 1cm$^2$(21.1) | Joule,2023, 7, 398-415 |
| n-i-p | spin-coating | 0.1cm$^2$(23.6) | 1cm$^2$(20.19) | The Innovation, 2022, 3.6 |
| p-i-n | blade-coating | / | 36cm$^2$(15.17) | Nature Communications, 2020, 11: 3016. |

| | | | | |
|---|---|---|---|---|
| **n-i-p** | **spin-coating** | **0.09cm$^2$(24.51)** | **10cm$^2$(20.53)** | **This work** |

## References

[1] L. Chen, P. B. Ingabire, J. Sun, Z. Gu, J. Xi, L. Qiu, B. Bai, X. Yin, L. Song, J. Xiong, C. Cui, P. Du, *Adv. Funct. Mater.* **2025**, e21907.

[2] Y. Zhang, T. Kong, H. Xie, J. Song, Y. Li, Y. Ai, Y. Han and D. Bi, ACS Energy Lett. 2022, 7, 929-938.

[3] G. Liu, H. Zheng, J. Ye, S. Xu, L. Zhang, H. Xu, Z. Liang, X. Chen and Xu Pan, ACS Energy Lett. 2021, 6, 4395-4404.